

# High Beta and High Density Operation in TPE-RX<sup>\*</sup>)

Haruhisa KOGUCHI, Hajime SAKAKITA, Satoru KIYAMA,  
Kiyoyuki YAMBE, Tomohiko ASAI<sup>1)</sup>, Yoichi HIRANO,  
Fulvio AURIEMMA<sup>2)</sup>, David TERRANOVA<sup>2)</sup> and Paolo INNOCENTE<sup>2)</sup>

*Energy Technology Research Institute (ETRI), National Institute of Advanced Industrial  
Science and Technology (AIST), Tsukuba, Ibaraki 305-8568, Japan*

<sup>1)</sup>*College of Science and Technology, Nihon University, Tokyo 101-8308, Japan*

<sup>2)</sup>*Consorzio RFX, Associazione Euratom-ENEA sulla Fusione, corso Stati Uniti 4, 35127 Padova, Italy*

(Received 14 January 2009 / Accepted 11 March 2009)

A high poloidal beta,  $\beta_p$ , was achieved using pulsed poloidal current drive (PPCD) in a toroidal pinch experiment-RX (TPE-RX). The plasma electron density and temperature increased, hence improving  $\beta_p$  from 5 to 30% during PPCD.  $\beta_p$  is almost equal to the total beta in the reversed-field pinch (RFP). D-alpha emission from recycling deuterium by the plasma-wall interaction decreased during the PPCD. An improved particle confinement time was indicated by a ten fold increase in the ratio of the total number of particles to the D-alpha emission. Single pellet injection into the good particle confinement plasma, achieved by the PPCD, produced high density plasma with high beta values. The plasma electron density rapidly increased to triple that of standard plasma, and high density was maintained till the end of the PPCD period. The electron temperature was lower than that of PPCD without ice pellet injection, but  $\beta_p$  remained almost the same because the plasma electron density was higher with pellet injection.

© 2009 The Japan Society of Plasma Science and Nuclear Fusion Research

Keywords: reversed-field pinch (RFP), pulsed poloidal current drive (PPCD), high-beta plasma, pellet injection

DOI: 10.1585/pfr.4.022

## 1. Introduction

Toroidal pinch experiment-RX (TPE-RX) is one of the three largest reversed-field pinch (RFP) devices, with major and minor radii of 1.72 and 0.45 m, respectively [1]. Due to limitations in its power supply, TPE-RX is operated at less than 500 kA. High beta operation is one of the design concepts of RFP plasma used as a simple fusion device. The global confinement properties under the standard discharge of TPE-RX and at less than 500 kA give poloidal beta,  $\beta_p$ , range of 5-10%. The  $\beta_p$  value is almost equal to the total beta in the RFP device. The standard discharge is characterized by gas fueled by a steady flow of deuterium and the pinch parameter,  $\theta$ , controlled in the range of 1.4-1.5. Here, the pinch parameter is a control parameter of the RFP device, and is defined as the ratio of the poloidal magnetic field at the plasma surface to the averaged toroidal magnetic field. Equilibrium is maintained by a thick conducting shell and a feedback-controlled error field compensation at the poloidal gap. In the RFP configuration, the main component of the magnetic field at the plasma surface is the poloidal magnetic field, and the toroidal magnetic field is in the direction opposite from the toroidal magnetic field at the plasma center. The main component of the plasma current near the plasma surface

is in the poloidal direction, and only a toroidal one-turn voltage is applied externally by a flux swing in the standard RFP plasma. Therefore, the poloidal plasma current is maintained by the plasma itself through non-linear coupling between the magnetic and velocity fluctuations. The mechanism for generating the effective electromotive force parallel to the average magnetic field is referred to as a dynamo effect [2]. The dynamo effect plays important roles in sustaining the RFP configuration and in transporting the plasma particles, due to the stochastic magnetic field.

There are several operating conditions differing from the standard discharge, which improve the confinement properties. In TPE-1RM20 device (an immediate predecessor of TPE-RX) the stored energy,  $\beta_p$ , and energy confinement time all were doubled at a high  $\theta$  discharge, under particularly clean wall conditions [3]. Magnetic fluctuations decreased to about one-third and  $\beta_p$  increased to about 18% at  $\theta = 2.0$ . Pulsed poloidal current drive (PPCD), which was first introduced in MST [4], is another operating method for obtaining improved confinement in the RFP device [4-9]. PPCD has been investigated in many RFP devices and is an extremely powerful technique as it reduces the dynamo effect by directly driving the poloidal current with adequate control of the external toroidal field coil current [8, 9]. In TPE-RX, the PPCD power supply was upgraded and the PPCD period lengthened.

The plasma electron density of TPE-RX is low com-

author's e-mail: h-koguchi@aist.go.jp

<sup>\*</sup>) This article is based on the invited talk at the 24th JSPF Annual Meeting (2007, Himeji).

pared with those of the other RFP devices. The density in the standard TPE-RX discharge shows an almost linear dependence on the plasma current. Controlling the plasma electron density with the same current is a major issue in TPE-RX. Gas puffing was conducted in TPE-RX, and plasma electron density could be increased five fold [10]. The fast valve for gas puffing is located at two toroidal positions and the density is controlled by changing the back pressure of the gas puffing systems. Magnetic fluctuation also increased, probably because of edge cooling caused by the neutral gas. In order to control the plasma electron density with less edge cooling, an ice pellet injection experiment was conducted [11]. Here, we present the experimental results when an ice pellet is injected into the PPCD plasma. A marked density increase during PPCD by ice pellet injection was observed.

This paper is organized as follows. In Sec. 2, we present the improved confinement properties obtained by the newly upgraded PPCD system. The confinement properties under ice pellet injection will be discussed in Sec. 3.

## 2. Pulsed Poloidal Current Drive in TPE-RX

### 2.1 Operating conditions for PPCD discharge

Figure 1 shows the waveform of the plasma current,

$I_p$ , the toroidal magnetic field at outside of the wall,  $B_{\text{tout}}$ , the toroidal magnetic field at the plasma surface,  $B_{\text{ta}}$ , the total toroidal magnetic flux, and the electric field parallel to the magnetic field at the plasma surface,  $E_{\parallel}$ .  $E_{\parallel}$  is estimated by

$$E_{\parallel} = \mathbf{E}(a) \cdot \mathbf{B}(a) / |\mathbf{B}(a)|$$

$$= [(V_{\text{ta}}/2\pi R)B_{\text{ta}} + (V_{\text{pa}}/2\pi a)B_{\text{pa}}] / (B_{\text{ta}}^2 + B_{\text{pa}}^2)^{1/2}.$$

Here,  $\mathbf{E}(a)$  is an electric field at the plasma surface.  $V_{\text{ta}}$  and  $V_{\text{pa}}$  are the toroidal and poloidal one-turn voltages at the plasma surface, respectively.  $R$  and  $a$  are the major and minor radii, respectively.  $\mathbf{B}(a)$  the magnetic field at the plasma surface, and  $B_{\text{pa}}$  the poloidal magnetic field at the plasma surface ( $B_{\text{pa}} = \mu_0 I_p / (2\pi a)$ ).  $E_{\parallel}$  is usually negative in a standard discharge, and the effective electromotive force sustaining the RFP configuration is maintained by a self-organization process (dynamo activity). Since a positive  $E_{\parallel}$  value can drive the poloidal current density, which sustains the toroidal magnetic field configuration of the RFP, it assists self-organization by the effective electromotive force parallel to the average magnetic field. The dynamo activity can be reduced when  $E_{\parallel}$  is positive [8, 9]. The red line in each figure indicates the waveform for a standard discharge of  $I_p = 300$  kA, while the blue lines indicate the PPCD discharge waveform. The plasma duration is about 70 ms in the standard discharge and 35 ms in the PPCD discharge, as shown in Fig. 1 (a).

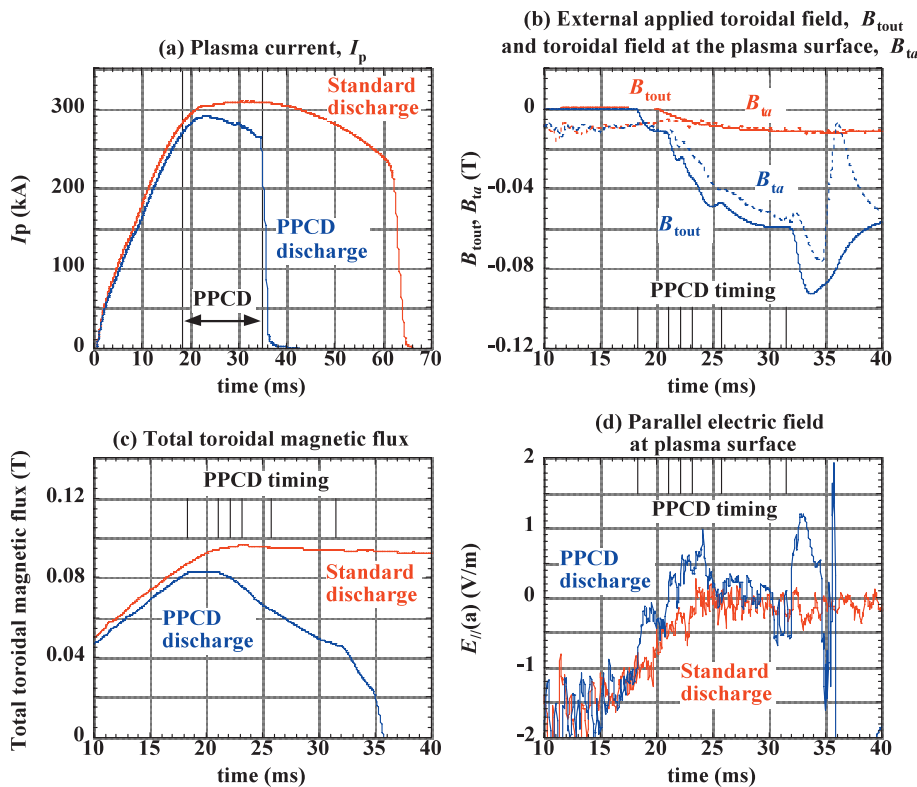


Fig. 1 Plasma current (a), toroidal magnetic field at outside of the wall (solid line in (b)), toroidal magnetic field at the plasma surface (dashed line in (b)), total toroidal magnetic flux (c), and parallel electric field to the magnetic field at the plasma surface (d).

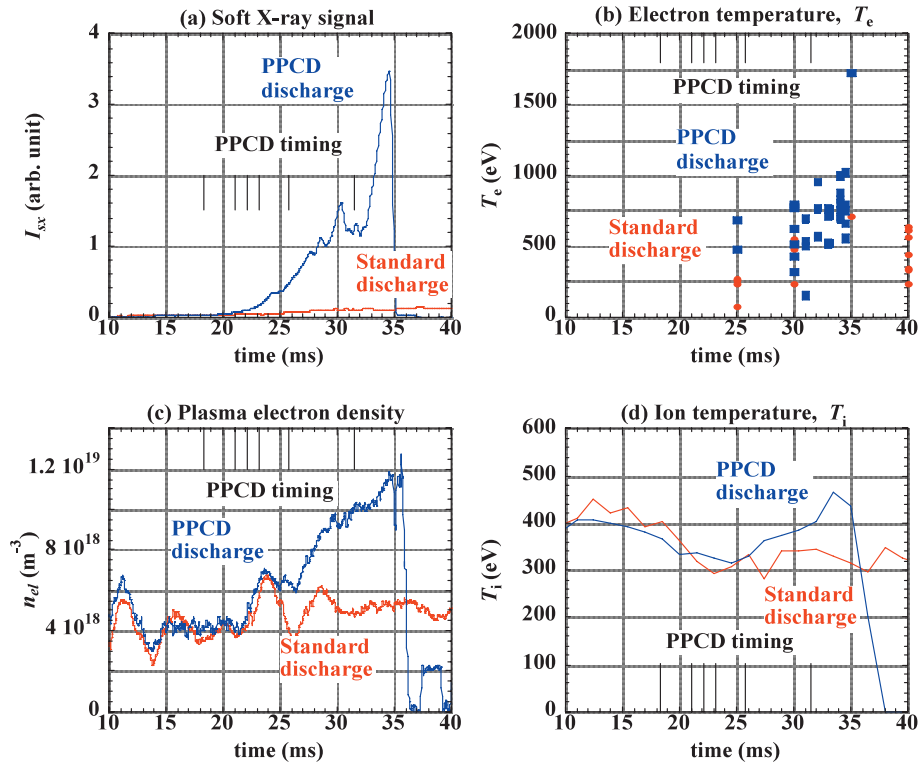


Fig. 2 Soft X-ray signal (a), plasma electron temperature at plasma center (b), plasma electron density (c), and ion temperature (d).

Figure 1 (b) indicates  $B_{\text{tout}}$  with a solid line and  $B_{\text{ta}}$  with a dashed line.  $B_{\text{ta}}$  is generated by external coil current and also by an induced current in the liner. The poloidal one-turn voltage is induced by a change in the total toroidal magnetic flux. The total toroidal magnetic flux increases during the ramp up phase ( $< 20$  ms, as shown in Fig. 1 (c)) and induces a poloidal current in the liner. The reversal field is self-organized without  $B_{\text{tout}}$ , as indicated by the dashed line in Fig. 1 (b). In a standard plasma,  $E_{\parallel}$  is usually negative during the ramp up phase and approximately zero during the flattop phase ( $t = 20 \sim 40$  ms), as shown in Fig. 1 (d). The PPCD power supply in TPE-RX consists of six groups of capacitor banks. The PPCD waveform is controlled to achieve the best results. We control the timing and charging voltage of each capacitor bank to maintain a positive value for  $E_{\parallel}$  as long as possible. Optimized PPCD timing is shown in Figs. 1 (b)-(d).  $B_{\text{tout}}$  is stepped down six times and the total toroidal magnetic flux decreases smoothly. The total toroidal magnetic flux decreases after applying the PPCD and the poloidal electric field is induced.  $E_{\parallel}$  increases rapidly and becomes positive, as shown in Fig. 1 (d).  $E_{\parallel}$  is kept positive during the PPCD and the soft X-ray signal,  $I_{\text{SX}}$ , increased ten fold, as shown in Fig. 2 (a), thus indicating that the confinement properties were improved.

## 2.2 Plasma diagnostics for PPCD plasma

A Thomson scattering system, using Nd-Yag laser

and a polychromator, was installed in TPE-RX. This is a single-pulse laser system that can measure the plasma electron temperature,  $T_e$ , at the plasma center. Red symbols in Fig. 2 (b) denote  $T_e$  for a standard discharge, and each point is measured by one discharge under the same operating conditions. The ensemble averaged  $T_e$  is about 428 eV at  $t = 30$  ms. Blue symbols denote  $T_e$  for the PPCD discharge.  $T_e$  increases rapidly during the PPCD and the ensemble averaged  $T_e$  increases to 834 eV at  $t = 34$  ms, as suggested by the increase in  $I_{\text{SX}}$ . The maximum  $T_e$  is 1730 eV in this experiment. The ensemble averaged  $T_e$  at  $t = 40$  ms is almost the same at  $t = 30$  ms and  $T_e$  is almost constant during the flattop phase in a standard discharge.  $T_e$  increases more than two fold at the end of the PPCD. The electron density profile is measured using a double-chord CO<sub>2</sub>/HeNe laser interferometer, whose impact parameters, normalized by  $a$ , are 0.0 and 0.69 [10]. Figure 2 (c) shows the line averaged plasma electron density along the center chord ( $r/a = 0.0$ ),  $n_{e\ell}$ .  $n_{e\ell}$  in a standard discharge is about  $5 \times 10^{18} \text{ m}^{-3}$ , as indicated by the red line.  $n_{e\ell}$  in a PPCD discharge increases gradually during the PPCD period, reaching two fold higher than  $n_{e\ell}$  in standard operation ( $1 \times 10^{19} \text{ m}^{-3}$ ) at the end of the PPCD. It is considered that the particle confinement is improved greatly. The ion temperature at the plasma center,  $T_i$ , measured by the NPA system is shown in Fig. 2 (d).  $T_i$  in the standard discharge decreases slowly and is about 300 eV at  $t = 35$  ms, as shown by the red line.  $T_i$  in the PPCD discharge increases to 450 eV, as shown by the blue line.

$T_e$  is almost the same as  $T_i$  in a standard discharge, but  $T_e$  becomes twice as high as  $T_i$  in a PPCD discharge.

### 2.3 Confinement properties in PPCD

The results of  $T_e$ ,  $T_i$ , and  $n_{el}$  measurements indicate that the confinement properties are improved during the PPCD operation. We evaluated the particle confinement and poloidal beta values. Here, we note that the main component of the magnetic field at the plasma surface is the poloidal magnetic field. Thus, the poloidal beta is almost equal to the total beta in the RFP.

As shown in Fig. 2 (c), a gradual increase of  $n_{el}$  is observed during the PPCD operation. Simultaneously, the radiation intensity corresponding to the  $D\alpha$  line,  $I_{D\alpha}$ , decreases significantly as shown in Fig. 3 (a). In order to measure the toroidal distribution of  $D\alpha$  emission, bundle fibers with a focusing lens were distributed in the toroidal direction. TPE-RX has sixteen port sections distributed equally around the toroidal direction (toroidally separated by  $22.5^\circ$  with respect to each other). The bundle fibers were installed at the inner equatorial port of the TPE-RX and their line of sight is along the major radius. Using this system,  $D\alpha$  line intensities are monitored at thirteen of the sixteen port sections.  $D\alpha$  emission is usually localized at the plasma surface and is higher at the outer side than at the inner side when the localized slinky structure is absent due to magnetic perturbation (called the locked mode). However, the difference between the emissions is not large. The observed  $D\alpha$  emission is averaged along the line of sight, including the inner and outer sides. The effect of poloidal asymmetry on  $D\alpha$  measurement should be small. The toroidal asymmetry of  $D\alpha$  emission is well correlated with the presence of the locked mode and its location [12]. The distribution of  $D\alpha$  emission is broad and without a peak when the slinky structure of the locked mode is absent. When a slinky structure exists,  $D\alpha$  emission is strongest at the center of the slinky structure of the locked mode [12].  $I_{D\alpha}$  includes the effect of the toroidal asymmetry of the  $D\alpha$  emission. Therefore,  $I_{D\alpha}$  can be considered proportional to the total influx of deuterium.  $I_{D\alpha}$  decreases by one-tenth during 2-3 ms at the end of the PPCD. In order to estimate the total number of electrons,  $N$ , we assumed the following electron density profile:  $n(r) = n_0[1 - (r/a)^4][1 + A(r/a)^4]$ . Here,  $n_0$  and  $A$  were determined by the two measured chord values. During the PPCD,  $N$  increases slowly and  $I_{D\alpha}$  decreases.  $D\alpha$  line emission is almost proportional to the amount of recycling deuterium from the first wall. The ratio of  $N$  to  $I_{D\alpha}$ , which approximately corresponds to the particle confinement time, is almost constant after  $t = 23$  ms in the standard discharge as shown by the red line in Fig. 3 (b).  $N/I_{D\alpha}$  increases significantly in the PPCD, by ten fold, as shown by the blue line in Fig. 3 (b).  $I_{D\alpha}$  has not been calibrated accurately, and hence  $N/I_{D\alpha}$  is an arbitrary unit. This improved particle confinement and the increase in  $T_e$  strongly

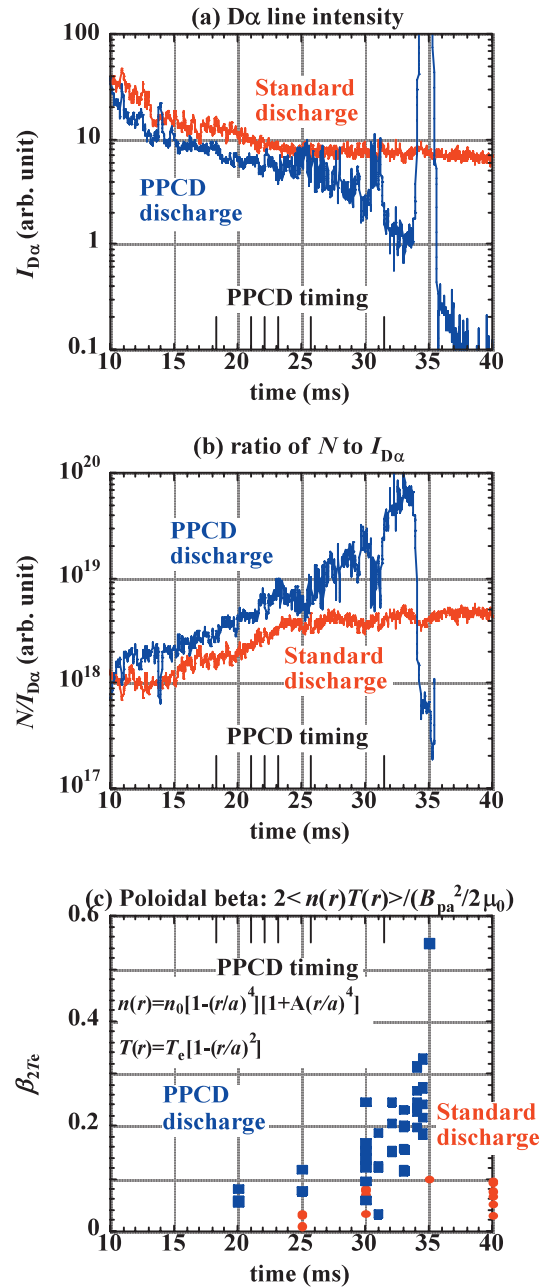


Fig. 3 Radiation intensity corresponding to the  $D\alpha$  line,  $I_{D\alpha}$  (a), ratio of total number of particles,  $N$  to  $I_{D\alpha}$  (b), and the time variations of  $\beta_{2Te}$  (c).

indicates a substantial improvement in the energy confinement.

Since the electron temperature profile has not been measured in TPE-RX, we assumed the temperature profile  $T(r) = T_e[1 - (r/a)^2]$  to discuss the poloidal beta.  $T_i$  should be included in the estimation of beta value, but the number of  $T_i$  measurements is not adequate to include in the present evaluation. We assume that  $T_i = T_e$ ,  $n_i = n_e$ , and the ion pressure profile to be same as the electron pressure profile. The beta value, including the measured  $T_i$ , will be discussed later.  $\beta_{2Te}$  is estimated from  $\beta_{2Te} =$

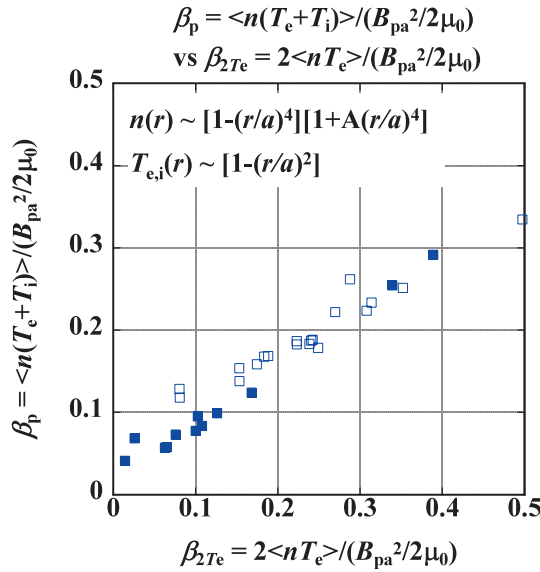


Fig. 4 The correlation between the electron poloidal beta,  $\beta_{2T_e}$  and actual poloidal beta,  $\beta_p$ . Open symbols indicate the pellet injection experiment.

$2\langle n(r)T(r) \rangle / (B_{pa}^2/2\mu_0)$ . Here,  $B_{pa}$  is the poloidal magnetic field at the plasma surface. The time variations of  $\beta_{2T_e}$  are plotted in Fig. 3 (c).  $\beta_{2T_e}$  in the standard shot is about 5% and is almost constant during the flattop phase, as shown by the red symbols in Fig. 3 (c).  $\beta_{2T_e}$  increases gradually during PPCD, as shown by blue symbols, and the ensemble averaged  $\beta_{2T_e}$  is 30% at  $t = 34$  ms. Increases in both  $T_e$  and  $n_e$  contribute to the attainment of this very high  $\beta_{2T_e}$  value. Background light emission that screens the scattered light increases just before the plasma crush. Therefore, it is difficult to measure  $T_e$  at  $t = 35$  ms. However, several data for  $T_e$  are available and  $\beta_{2T_e}$  increases until  $t = 35$  ms. The duration of the improved confinement becomes longer than 15 ms and high beta operation is achieved during all of the PPCD period.

Poloidal beta,  $\beta_{2T_e}$  increases to more than 40% at the end of the PPCD. This seems to be because the ion pressure is same as the electron pressure. Ion heating from PPCD is not remarkable, as shown in Fig. 2 (d).  $T_i$  is less than  $T_e$  at the end of PPCD and the ion pressure is less than the electron pressure. In order to estimate the actual  $\beta_p$ , we include the ion pressure in the estimation although the number of  $T_i$  measurements is not large. Figure 4 shows the correlation between the beta values including  $T_i$ ,  $\beta_p$ , and those estimated only by electron pressure,  $\beta_{2T_e}$ . Here,  $T_i$  measured by NPA is used as the ion temperature at the plasma center. The ion pressure is almost the same as the electron pressure in the low beta region and  $\beta_p$  almost equals  $\beta_{2T_e}$ . This is similar to the result in the standard discharge. Ion heating during the PPCD is usually small, and the ion temperature is about half of the electron temperature as described earlier.  $\beta_p$  is less than  $\beta_{2T_e}$  in the high  $\beta_{2T_e}$  region, and is about 30% at  $\beta_{2T_e} = 40\%$ . The

maximum  $\beta_p$  value is 34% in Fig. 4. Therefore, the actual achievable  $\beta_p$  in Fig. 3 (c) is estimated roughly to be about 30%. Here, we note that the electron temperature profile assumed in this estimation is narrower than that observed in other large RFP devices. Our estimation for beta value could be an underestimation—the real beta value seems to be higher.

Analysis of the RFP reactor indicates that a reactor design with a realistic  $I_p$  value and confinement property could be possible when  $\beta_p$  higher than 20% is realized [13]. A higher  $\beta_p$  is preferable because it results in a design with lower  $I_p$ . This  $\beta_p$  value of  $\sim 30\%$  can be considered as a milestone in the development of RFP research.

### 3. Deuterium Ice Pellet Injection in TPE-RX

A pellet injector, which was earlier used in the ETA-BETA II device [14], was installed in the TPE-RX. The specifications of the pellet injector are such that a pellet typically contains  $1 \times 10^{20}$  deuterium atoms and the injection velocity of the pellet can be as high as 400 m/s. The number of atoms can vary considerably in each shot, since pellet size reproducibility is poor. For each TPE-RX discharge, only a single pellet is launched into the plasma. The volume of the TPE-RX discharge is about  $7 \text{ m}^3$  and the expected maximum density increase is about  $1.4 \times 10^{19} \text{ m}^{-3}$ . The pellet is launched in the radial direction from the horizontal port. The pellet trajectory is measured by a position sensitive detector (PSD) [15]. PSD measures the projection of the pellet trajectory on the surface of a photo diode. It is installed next to the launch nozzle looking at the pellet from behind, such that the PSD measures only the deflection of the trajectory. The pellet is injected into the plasma in the off axis direction and is deflected to the center of the plasma by the fast electrons in the edge region. The pellet penetrates into the center of the plasma with ablation.

The pellet was injected into the plasma at  $t = 23$  ms and the  $D\alpha$  line was emitted impulsively for a few ms. The density increased quickly at both measurement chords after pellet injection (at  $t = 23$  ms). The density reached  $1.5 \times 10^{19} \text{ (m}^{-3}\text{)}$  at the center chord and  $2.7 \times 10^{19} \text{ (m}^{-3}\text{)}$  at the edge chord. The density profile became hollow, but the density at edge chord decreased much faster than that at the central chord shortly after the pellet ablation. This indicates that the density profile is flattened as in a standard PPCD. The value of  $N$ , estimated from the density profile function, is denoted by a black line in Fig. 5 (a). The blue and red lines denote the PPCD and standard discharge without a pellet, respectively. With the pellet,  $N$  increased to  $1.5 \times 10^{20}$  atoms and then decreased to  $1.2 \times 10^{20}$  atoms within a few ms. However,  $N$  did not decrease much at 6 ms and then increase again, as in the case of normal PPCD without a pellet.  $N$  tripled compared to the standard discharge at  $t = 32$  ms and quadrupled at the

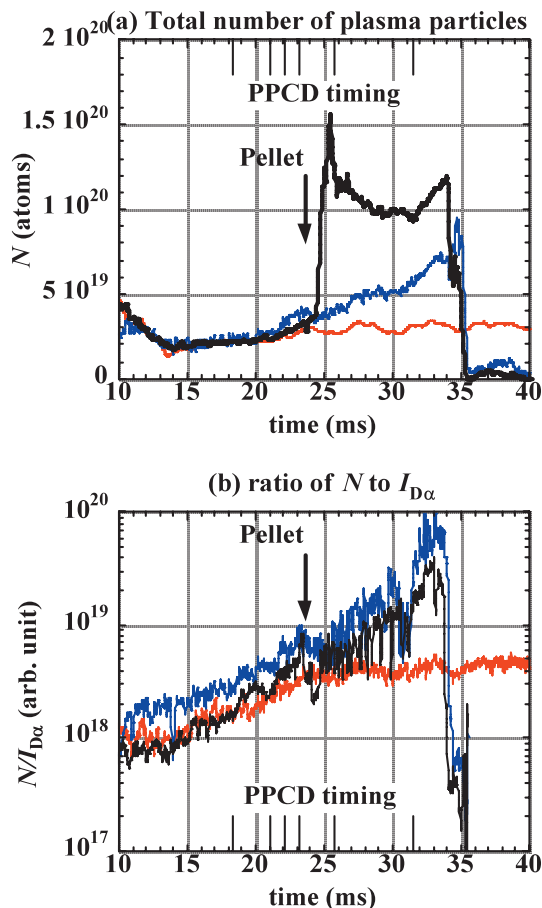


Fig. 5 Total number of plasma particles,  $N$ , estimated from the double chord interferometer (a), and the ratio of  $N$  to  $I_{D\alpha}$  correlated to particle confinement (b).

end of the PPCD.  $N/I_{D\alpha}$  decreased shortly after the pellet injection, but soon recovered to a level similar to that of the PPCD without a pellet, as shown by a black line in Fig. 5 (b).  $N/I_{D\alpha}$  is lower than that in the PPCD, but still remains adequate to demonstrate a significant improvement in the particle confinement during PPCD, even with pellet injection.

The open symbols in Fig. 4 show  $\beta_p$  during the PPCD discharge with pellet injection.  $\beta_p$  is still high with pellet injection, about 34%, which is similar to  $\beta_p$  for PPCD without pellet injection. Thus, the deuterium ice pellet injection during PPCD achieves high-density operation with improved confinement in 300 kA plasmas.

#### 4. Conclusion

This paper shows the result of high beta operation using PPCD in the TPE-RX and RFP device. The power supply for the PPCD was upgraded to six stage pulses of a reversed toroidal field. The poloidal beta value increased to 30% at the end of the PPCD. The electron temperature at the plasma center doubled and the maximum value

obtained in this experiment was 1730 eV. The line averaged plasma electron density also doubled, and was  $1.0 \times 10^{19} \text{ m}^{-3}$  at the end of the PPCD. Increase in the ratio of the total number of plasma electrons to the  $D\alpha$  emission indicates that dynamo activity and particle transport due to the stochastic magnetic field are reduced during the PPCD. During PPCD, the ion temperature increased by 1.5 times to 450 eV. This significant increase in the ion temperature has not been observed during PPCD in other RFP devices. The ion heating mechanism needs to be confirmed in further studies, including the equilibrium analysis. This paper also showed the results of density control using pellet injection. The poloidal beta in the pellet injection experiment during the PPCD is as high as in the PPCD and the maximum value is more than 30%. The ratio of the total number of plasma electrons to the  $D\alpha$  emission is almost same as in the PPCD. This indicates that PPCD with pellet injection achieves high beta and high density operation with good particle confinement.

#### Acknowledgements

The authors are grateful to the MST group, particularly to Prof. S. C. Prager, Dr. D. J. DenHartog, and Dr. R. O'Connell, for their valuable help and advice in the Thomson scattering measurements. We also thank Dr. T. Hatae of JAEA for his help in calibrating the Thomson scattering system. This study was financially supported by the Budget for Nuclear Research of the Ministry of Education, Culture, Sports, Science, and Technology of Japan, based on screening and counseling by the Atomic Energy Commission.

- [1] Y. Yagi, S. Sekine *et al.*, Fusion Eng. Des. **45**, 409 (1999).
- [2] H.A.B. Bodin and A.A. Newton, Nucl. Fusion **20**, 1255 (1980).
- [3] Y. Hirano *et al.*, Nucl. Fusion **36**, 721 (1996).
- [4] J.S. Sarff *et al.*, Phys. Rev. Lett. **72**, 3670 (1994).
- [5] D.J. Den Hartog *et al.*, Proc. 21st IAEA Fusion Energy Conference (Chengdu, China 2006) EX/8-2.
- [6] H. Koguchi *et al.*, Proc. 21st IAEA Fusion Energy Conference (Chengdu, China 2006) EX/P3-8.
- [7] S. Martini *et al.*, Proc. 21st IAEA Fusion Energy Conference (Chengdu, China 2006) EX/7-3.
- [8] L. Frassinetti *et al.*, Phys. Plasmas **11**, 5229 (2004).
- [9] B.E. Chapman, A.F. Almagri, J.K. Anderson *et al.*, Phys. Plasmas **9**, 2061 (2002).
- [10] A. Canton *et al.*, Plasma Phys. Control. Fusion **46**, 23 (2004).
- [11] H. Koguchi *et al.*, Jpn. J. Appl. Phys. **45**(42), L1124 (2006).
- [12] D. Pasqualini *et al.*, J. Phys. Soc. Jpn., **75**, No.2, 023501 (2006).
- [13] Y. Hirano, J. Plasma Fusion Res. **77**, 793 (2001), in Japanese.
- [14] H. Sorensen *et al.*, Proc. 14th Symp., Fusion Technology, Avignon (1986) p.1355.
- [15] P. Innocente *et al.*, Rev. Sci. Instrum **70**, 943 (1999).